Journal of Fluorescence, Vol. 7, No. 2, 1997

Saturation Effects on Phosphorescence Anisotropy Measurements at High Laser Pulse Energies

Haitao Peng[1] and B. George Barisas[1,2]

Received July 25, 1996; accepted April 14, 1997

Triplet spectroscopic methods such as time-resolved phosphorescence anisotropy permit successful measurement of slow rotational diffusion of membrane proteins. However, these methods are potentially subject to saturation phenomena. We present theoretical and experimental studies of how high excitation energy densities can complicate measurements of phosphorescence intensity and anisotropy. Increases in excitation laser pulse energy initially increase phosphorescence intensity. Further increases then lead to phosphorescence saturation. As a consequence, the initial phosphorescence anisotropy decreases and approaches zero at very high excitation energies. The relative standard deviation of anisotropies measured in any system reaches a minimum at some particular excitation energy density. These results allow us to define optimum experimental conditions for time-resolved phosphorescence anisotropy measurements. For example, for excitation of erythrosin chromophores at typical wavelengths by the center of a Gaussian laser beam, optimum pulse energies in microjoules are approximately 5.0 R^2, where R is the beam $1/e^2$ radius in mm.

KEY WORDS: Phosphorescence; anisotropy; triplet; saturation; membrane; rotation.

INTRODUCTION

Integral membrane proteins play important roles in cellular activation, adhesion, metabolism, transport, and hormonal regulation.[1-3] Within the membrane, these proteins exhibit both translational and rotational Brownian diffusion. Rotational diffusion, typically occurring on the microsecond time scale, is of special interest because it is particularly sensitive to the size and environment of proteins. Various optical methods have been developed to measure protein rotational diffusion.[4-6] Most such methods involve the use of triplet-forming chromophores such as eosin or erythrosin, which exhibit triplet lifetimes at least as long as the rotational phenomena of interest. The best known of these methods, time-resolved phosphorescence anisotropy (TPA),[7] uses phosphorescent dyes such as erythrosin isothiocyanate conjugated to an antibody, lectin, or hormone, which binds the membrane protein of interest. The linearly polarized output from a pulsed laser is used to excite phosphorescence from properly oriented label chromophores. Initially, phosphorescence is weakly polarized in the plane of polarization of the exciting light, but this polarization decays as rotational motion randomizes chromophore orientation prior to phosphorescence emission. This decay, quantitated by the emission anisotropy function, is analyzed to obtain the rotational parameters of interest.

In our use of TPA, we have found that this method is subject to saturation phenomena. Excitation with unnecessarily low laser pulse energies yields weak phosphorescence signals and high noise levels in anisotropy traces. On the other hand, excessive excitation energies will lead to saturation of ground state chromophores, artifactually low anisotropies and high relative errors in anisotropy measurements. Identification of correct exci-

[1] Department of Chemistry, Colorado State University, Fort Collins, Colorado 80523.

[2] To whom correspondence should be addressed.

1053-0509/97/0600-0139$12.50/0

tation energies can thus help to obtain optimum phosphorescence anisotropy data. Although saturation of phosphorescence was noted by Jovin *et al.*,[8,9] theoretical and experimental investigations of this phenomenon have not been reported. Burghardt[21] has discussed the somewhat related topic of saturation effects on polarized photobleaching measurements of slow protein rotational motion.

THEORY

A sample containing triplet-forming chromophores is irradiated with a brief pulse of vertically polarized light. Those molecules whose absorption transition dipoles are aligned parallel to the excitation polarization will be preferentially excited. This creates an anisotropic distribution of singlet excited state chromophores which then undergo intersystem crossing to the triplet state. Relaxation from the triplet state to the singlet ground state results in phosphorescence. When an emission polarizer is placed parallel or perpendicular to the excitation pulse, the detected emission intensities are $I_{\parallel}(t)$ and $I_{\perp}(t)$, respectively. The total emission intensity s(t) and anisotropy r(t) can be calculated as

$$s(t) = I_{\parallel} + 2I_{\perp} \tag{1}$$

$$r(t) = [I_{\parallel}(t) - I_{\perp}(t)]/s(t) \tag{2}$$

By measuring $I_{\parallel}(t)$ and $I_{\perp}(t)$ over time, time-resolved anisotropy can be calculated and its decay evaluated. During the lifetime of the triplet excited state, molecules rotate and orientation of the molecular emission dipoles is randomized. Thus the measured anisotropy decays from the initial value r_0 to zero. This decay can often be satisfactorily represented as a single-exponential process,

$$r(t) = r_\infty + (r_0 - r_\infty)e^{-t/\phi} \tag{3}$$

where r_0 is the initial anisotropy, r_∞ is the limiting anisotropy, and ϕ is the rotational correlation time. It is well-known that the initial anisotropy r_0 can be as high as 2/5,[10] but measured values are typically much lower. An ultimate limit is set by the angle γ between the chromophore's absorption and emission dipoles since $r_0 \leq (2/5)P_2(\cos\gamma)$, where the second-order Legendre polynomial $P(\cos\theta)$ is $1/2(3\cos^2\theta - 1)$. However, the actual initial anisotropy measured in a typical TPA experiment is substantially reduced below this photophysical limit by chromophore motion relative to the protein and by protein segmental motions, both occurring on a nanosecond time scale before observation can begin. We show below that optical saturation can also markedly reduce apparent anisotropies.

When a photon of appropriate excitation wavelength impinges on a molecule where the angle between the light polarization and the molecular absorption transition dipole is θ, the probability P of the photon being absorbed is

$$P(\theta) = 1 - e^{-a\cos^2\theta} \tag{4}$$

where the reduced excitation energy density a is calculated as

$$a = \frac{3000(\ell n10)\,\varepsilon\lambda\Phi w}{hcN} \tag{5}$$

Among the constants in Eq. (5), h is Planck's constant, c is the speed of light, N is Avogadro's number, ε is the molar absorptivity of the chromophore, λ is the excitation wavelength, Φ is the chromophore's overall quantum yield for triplet formation, and w is the energy density. If excitation occurs at the center of a Gaussian laser beam, w is calculated as $2E/(\pi R^2)$, where E is the laser pulse energy and R is the $1/e^2$ beam radius. Inspection of Eq. (4) shows that molecules whose absorption transition dipoles are parallel to the polarized excitation have the highest probability of being excited. However, the probability of exciting molecules whose transition dipoles reside at large angles with respect to the plane of polarization increases as the pulse energy increases.

For purposes of this paper we assume that the chromophore's absorption and phosphorescence emission dipoles are coincident, i.e., that $\gamma = 0$. This is a reasonable approximation for xanthine dyes such as erythrosin; and in any case, we are interested only in how the real anisotropy, whatever it may be, is affected by saturation. At times immediately after excitation, the two measured initial phosphorescence intensities $I_{0\parallel}$ and $I_{0\perp}$ depend upon the excitation probability $P(\theta)$ of variously oriented molecules, upon the number n of molecules excited, upon the efficiency ε of detection and upon the rate constant k_p for phosphorescence as

$$I_{0\parallel}(a) = \frac{1}{2} n\varepsilon k_p \int_0^{\pi} P(\theta)\cos^2\theta\sin\theta\, d\theta \tag{6}$$

$$I_{0\perp}(a) = \frac{1}{4} n\varepsilon k_p \int_0^{\pi} P(\theta)\sin^2\theta\sin\theta\, d\theta \tag{7}$$

Upon evaluation of these integrals, the initial intensities are expressed as

$$I_{0\parallel}(a) = n\varepsilon k_p \{\frac{1}{3} + \frac{e^{-a}}{2a} - \frac{1}{4a}\sqrt{\frac{\pi}{a}}\,\mathrm{erf}(\sqrt{a})\} \quad (8)$$

$$I_{0\perp}(a) = n\varepsilon k_p \{\frac{1}{3}\frac{e^{-a}}{4a} - \frac{2a-1}{8a}\sqrt{\frac{\pi}{a}}\,\mathrm{erf}(\sqrt{a})\} \quad (9)$$

where

$$\mathrm{erf}(\sqrt{a}) = \frac{2}{\sqrt{\pi}}\int_0^{\sqrt{a}} e^{-x^2}\,dx \quad (10)$$

These equations allow calculation of the initial emission intensity s_0 and the initial anisotropy r_0 as

$$s_0(a) = n\varepsilon k_p\,(1 - \frac{1}{2}\sqrt{\frac{\pi}{a}}\,\mathrm{erf}(\sqrt{a})) \quad (11)$$

$$r_0(a) = \frac{3e^{-a}}{2a} + \frac{2a-3}{4a}\sqrt{\frac{\pi}{a}}\,\mathrm{erf}(\sqrt{a})\Big/2 - \sqrt{\frac{\pi}{a}}\,\mathrm{erf}(\sqrt{a}) \quad (12)$$

We now calculate the effect of the excitation energy density on the relative standard deviation in measured anisotropies. If, for any time after excitation, we denote $I_\parallel - I_\perp$ by y and $I_\parallel + 2I_\perp$ by s, and let subscripted σ represent the standard deviations of the various variables, the relative error σ_r of the anisotropy is seen to be given by

$$\sigma_r/r = (\sigma_y^2/y + \sigma_s^2/s^2)^{\frac{1}{2}} \quad (13)$$

Since anisotropies are typically small, both $I_\parallel$ and $I_\perp$ can be approximated by $s/3$. If intensities are given as photon counts per channel, σ_s equals s since Poisson statistics apply. Moreover, $r^2 \ll 1$. Thus

$$\sigma_r/r = [(1 + \frac{2}{3}r^2)/s]^{\frac{1}{2}} \simeq [\frac{2}{3r^2s}]^{\frac{1}{2}} \quad (14)$$

The above results are also fully applicable to saturation effects in time-resolved fluorescence anisotropy measurements. However, the energy densities required for chromophore saturation are much less likely to be achieved in the picosecond excitation pulses typically employed in such experiments.

EXPERIMENTAL

Derivatization of Bovine Serum Albumin with Erythrosin Isothiocyanate. Bovine serum albumin (BSA; Sigma Chemical Co., St. Louis, MO) was derivatized with erythrosin isothiocyanate (ErITC; Molecular Probes, Eugene, OR) using the method described by Johnson and Holborow[11] to obtain a product with an ErITC/BSA molar ratio of approximately 1.0. One hundred microliters of 10^{-5} *M* ErITC–BSA in phosphate-buffered saline was added to 900 μl of 100% glycerol to obtain a 90% glycerol solution in which the concentration of ErITC–BSA was approximately 10^{-6} *M*. The actual percentage of glycerol in a sample was determined by measuring the refractive index and using standard tables.[12]

TPA Measurements. A block diagram of the TPA apparatus is shown in Fig. 1. The ErITC–BSA sample contained in a 5 × 5-mm Suprasil quartz cuvette was mounted in a thermostated cuvette holder. A temperature-controlled water bath was used to maintain the sample temperature at 20.5°C during each experiment. The 532-nm output of a Spectra-Physics DCR-11 Nd:YAG laser provided excitation pulses for the experiments. The laser was operated at 10 Hz with a vertically polarized TEM00 output. To obtain low laser energy densities, beam splitters were used in conjunction with mirrors to attenuate the beam. Laser pulse energy was measured by a Laser Probe Rm-3700 energy meter (Utica, NY) and the beam profile was determined by translating a slit or pinhole across the beam while recording transmitted energy. The $1/e^2$ radius of the beam was 3.9 mm, from which a 0.5-mm region was isolated by an iris for sample illumination. Phosphorescence emission from the sample was collected at 90° to the excitation axis. A 1 *M* sodium dichromate solution, a KV-550 barrier filter, and a 715-nm longpass filter were placed in front of the rotatable emission polarizer to eliminate exciting light. The phosphorescence signal was collected by an EMI 9816A photomultiplier tube (PMT). A fast gating circuit was used to gate the PMT off during the excitation laser pulses.[13,14] The output signal from the PMT was amplified by a Tektronix 476 oscilloscope and then by a 35-MHz bandwidth buffer amplifier. Two thousand forty-eight traces in each orientation were averaged by a Nicolet 12/70 signal averager and downloaded to a 80386 microcomputer for storage and analysis. To minimize the effects of any sample photobleaching and/or long-term fluctuations in laser intensity on measured anisotropies, these traces are collected as a sequence of 64-trace blocks with the emission polarizer in the parallel and perpendicular orientations in even- and odd-numbered blocks, respectively. In fact, almost no photobleaching of erythrosin is observed. For example, excitation of ErITC–BSA at a reduced excitation energy density of 1 causes only 0.64% phosphorescence loss after 2048 laser pulses (data not shown). If data are col-

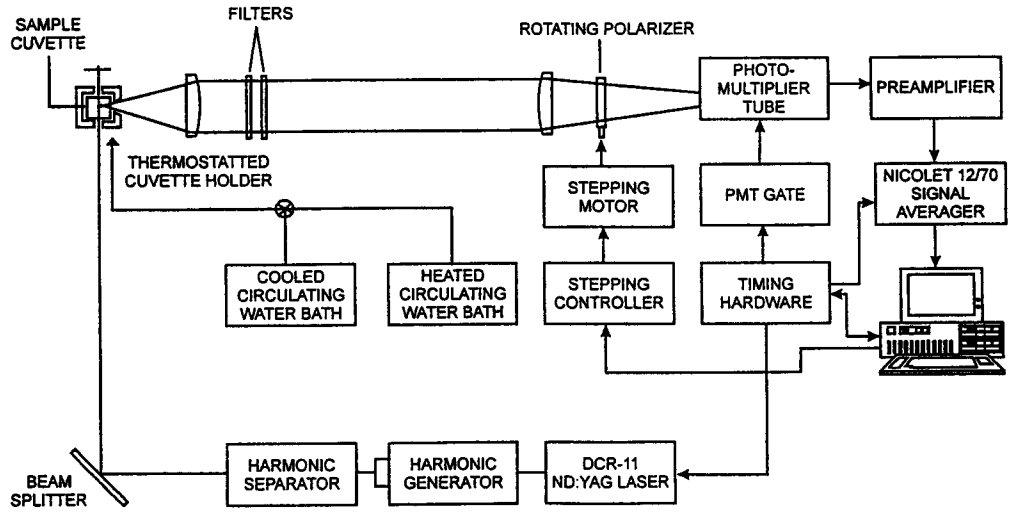

Fig. 1. Block diagram of apparatus for time-resolved phosphorescence anisotropy measurements. The functions of the various components are described in the text.

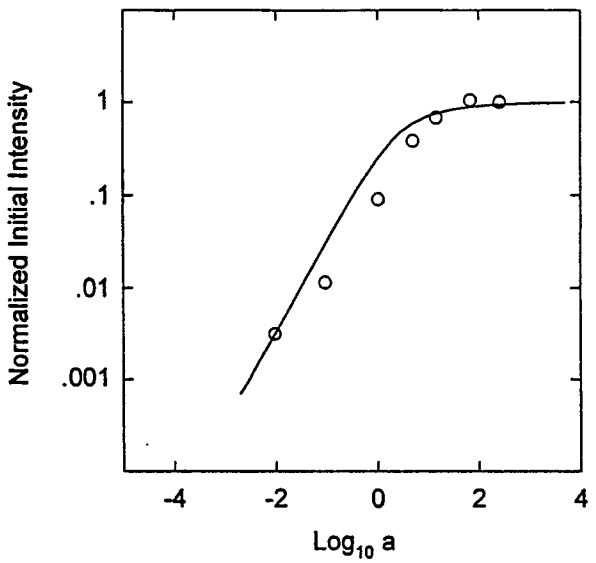

Fig. 2. Initial phosphorescence intensity, normalized to the highest value observed, plotted versus reduced laser energy density a for 1 μM ErITC–BSA in 90% glycerol solution at 20.5°C. a is defined by Eq. (5). The solid line represents theoretically calculated values from Eq. (11) and the open circles are experimental data points from Table I.

lected in blocks of 64 laser pulses as described above, such photobleaching increases measured anisotropies by less than 0.0007.

Data Analysis. Phosphorescence intensities $I_{\parallel}(t)$ and $I_{\perp}(t)$ were used to calculate a total emission intensity function $s(t)$, the decay of which was analyzed according to a two exponential model. Results from the lifetime analysis were used to weight anisotropy points in a nonlinear least-squares fit to Eq. (3) to obtain the initial anisotropy r_0, the limiting anisotropy r_∞, and the rotational correlation time ϕ, as well as the statistical uncertainties in these quantities.[15] The standard deviation of anisotropies measured near the beginning of the decay trace, *i.e.*, where $r(t) \propto r_0$, was calculated manually.

RESULTS AND DISCUSSION

Inspection of Eq. (11) shows how increasing excitation energy density a ought to affect initial phosphorescence intensity s_0. Phosphorescence should first increase, then approach saturation for large values of the reduced energy density a, as shown by the smooth curve in Fig. 2. Data in Table I were obtained when identical samples of ErITC–BSA in 90% glycerol were excited by laser energies extending over several orders of magnitude. In Fig. 2 these intensities, normalized to the highest value observed, are plotted *vs* a and compared with values calculated from Eq. (11). Good quantitative agreement is observed. For $a = 1$, the initial phosphorescence intensity is 25% of the maximum possible value and, at $a = 3$, it reaches 50%. s_0 plateaus at an essentially constant value when a exceeds about 10. Clearly, for evaluating kinetics of phosphorescence decay, there is little benefit in employing excitation energy densities above, say, $a \propto 1$.

Equation (12) predicts how initial anisotropies r_0 should be affected by high excitation energy densities.

Table I. Dependence of Phosphorescence Intensity and Anisotropy on Excitation Laser Energy Density[a]

E (μJ)[b]	w (μJ/cm²)[c]	a [ex Eq. (5)][d]	I_{phos}[e]	r_o[f]	s_{r0}/r_0[g] (×10⁴)
0.745	3.10	0.0096	0.0032	0.140	55.4
7.12	29.6	0.092	0.0116	0.140	35.0
79.9	332	1.03	0.091	0.123	14.8
390	1620	5.02	0.383	0.092	18.4
1140	4740	14.7	0.693	0.071	19.2
5360	22300	69.1	1.01	0.030	25.8
19900	82700	256	1.00	0.015	53.2

[a] The sample was 1 μ*M* ErITC–BSA, with a dye-to-protein molar ratio of 1.0, in 90% glycerol thermostated at 20.5°C. For each sample, 2048 $I_\parallel$ and $I_\perp$ traces were averaged and used to calculate the total emission and anisotropy functions.

[b] E is the total energy per excitation pulse in μJ.

[c] w is the excitation energy density in μJ/cm² calculated as $2E/(\pi r^2)$, where r is the $1/e^2$ radius of the laser beam.

[d] a is the reduced excitation energy density for excitation of erythrosin phosphorescence by 532-nm light calculated by means of Eq. (5) using values of 1.01×10^5 L mol^{-1} cm^{-1} and 1.0 for ε_M and Φ, respectively.

[e] I_{phos} is the initial phosphorescence intensity normalized to the highest value observed.

[f] r_0 is the initial anisotropy obtained by fitting experimental anisotropy decay curves to Eq. (3).

[g] s_{r0}/r_0 is the standard deviation of measured anisotropies in the initial portion of the decay curve divided by the fitted initial anisotropy. Results given are the means of three independent determinations.

The effect is easy to rationalize qualitatively. With increasing excitation the difference between $I_\perp$ and $I_\parallel$ decreases while s_0 plateaus. Thus the initial anisotropy falls and, in fact, approaches zero as the excitation energy density increases. Figure 3 presents initial anisotropies r_0 from Table I normalized to the maximum value observed and plotted *vs* the reduced energy density a. These are compared with values calculated from Eq. (12). Experimentally, r_0 decreases from 0.140 to 0.015 as a increases from 0.0096 to 256. Again, the observed dependence of initial anisotropy on excitation energy density is quantitatively described by the equations we develop. Calculation shows that, for $a = 1$, the initial anisotropy is 88% of the value observed at low excitation energy but that, by $a = 3$, it has decreased to only 70%. One might feel that excitation energies corresponding to $a \propto 1$ represent a reasonable upper limit for time-resolved phosphorescence anisotropy measurements since higher energies reduce anisotropies substantially.

The traces in Fig. 4 graphically underscore the severity of saturation effects on TPA measurements. For low reduced energy densities a, such as the value of 0.09 shown, both $I_\parallel$ and $I_\perp$ are proportional to a so that saturation effects on the initial anisotropy are negligible.

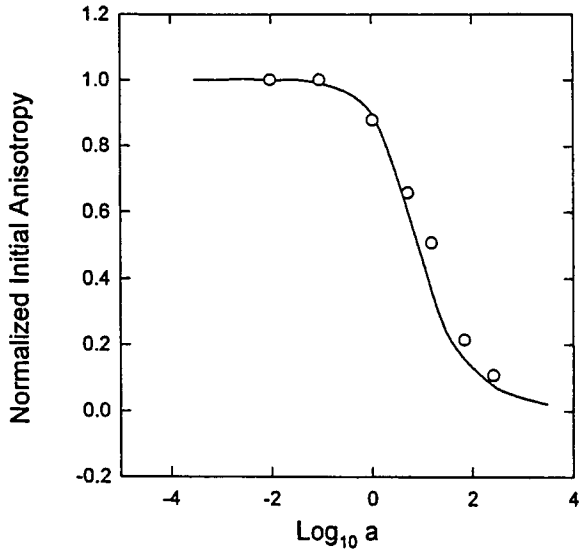

Fig. 3. Initial phosphorescence anisotropy, normalized to the highest value observed, plotted versus reduced laser energy density a for 1 μ*M* ErITC–BSA in 90% glycerol at 20.5°C. a is defined by Eq. (5). The solid line represents theoretically calculated values from Eq. (12) and the open circles are experimental data points from Table I.

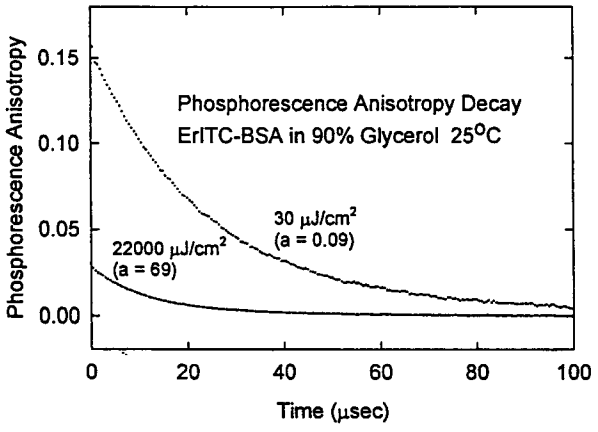

Fig. 4. Comparison of experimental time-resolved phosphorescence anisotropy traces obtained at low (a = 0.096) and high (a = 69) excitation energy densities on samples of ErITC–BSA in 90% glycerol at 20.5°C. The reduction of phosphorescence anisotropy by saturation is apparent in the high-energy trace.

As a increases beyond unity, such as to the value of 69 indicated, saturation of both $I_\parallel$ and $I_\perp$ causes these two quantities to approach each other, reducing apparent anisotropies. For example, the trace recorded at $a = 69$ exhibits anisotropies reduced almost fivefold by saturation.

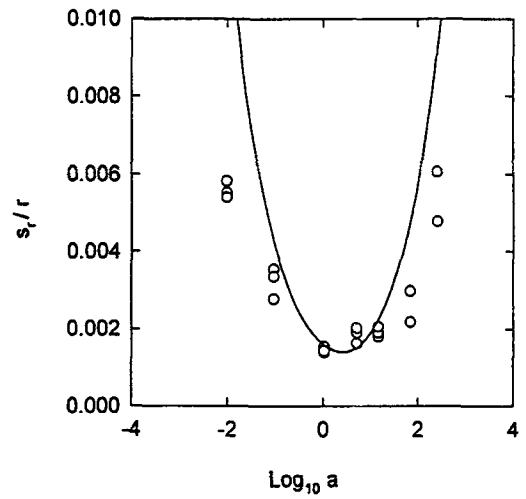

Fig. 5. Dependence of relative standard deviation of measured phosphorescence anisotropies on reduced laser energy density a defined by Eq. (5). Open circles are experimental points from Table I. The smooth curve is calculated by Eq. (14) and scaled to set the predicted minimum relative standard deviation equal to the minimum observed value. Such scaling is necessary since Eq. (14) assumes that intensities are determined by photon counting while we employ analog detection in practice. Thus a measured photocurrent reflects an indeterminate rate of photon counts and Eq. (14) needs to be multiplied by an appropriate constant to give relative standard deviations directly applicable to our experimental situation. We have simply chosen this constant so that the minimum relative standard deviation predicted by Eq. (14) agrees with the minimum value observed experimentally.

Equation (14) predicts the dependence of the relative standard deviation σ_r/r in measured anisotropies on a, assuming photon-limited noise. At very low excitation energy densities where s approaches 0 and $1/s$ approaches ∞, σ_r/r approaches ∞. At very high excitation levels where $I_\parallel$ approaches $I_\perp$ and r approaches 0, σ_r/r approaches ∞ once again. Between these two extremes a minimum relative error σ_r/r should be obtained at some value of a. Figure 5 compares measured relative standard deviations of measured phosphorescence anisotropies with those predicted by Eq. (14). This equation predicts that the noise-to-signal ratio in anisotropy measurements should attain a minimum at $a = 2.6$ and it is clear that the experimental noise-to-signal ratio reaches a minimum very close to this point. Moreover, the general shape of the experimental curve agrees satisfactorily with theory, though the minimum is somewhat shallower than might be expected. The likely explanation for this is that noise in our amplifiers is *not* solely photon-limited as Eq. (14) assumes but, rather, contains a constant component of electrical origin. In such a case an additional noise term would have to be added to Eq. (14), giving a higher minimum noise level and a broader minimum. If such a curve were lowered to superimpose its minimum upon the minimum of the experimental data, we would have the sort of curve shape observed.

We have thus investigated saturation effects on initial phosphorescence intensity and anisotropy at high laser excitation energy densities. At reduced excitation laser energy densities above ~1, phosphorescence intensities plateau and measured anisotropies begin to decrease rapidly. The minimum relative standard deviation of measured phosphorescence anisotropies occurs at $a = 2.6$, but at this excitation energy, anisotropies are reduced 30% by saturation. The tradeoff is thus between definition of the anisotropy decay curve, something optimized at $a = 2.6$, and agreement of measured anisotropies with their theoretically significant, low-excitation limiting values, something approached only with minimal excitation. We suggest that a reasonable compromise may be to operate near $a = 1$, where anisotropy values differ by at most 12% from those obtained in the low-excitation limit, while the decay curve signal-to-noise ratio is only marginally lower than the maximum obtainable at $a = 2.6$. Optimum experimental conditions for anisotropy measurements can thus be found from Eq. (5) and depend both upon the laser beam profile and on what part of the beam illuminates the sample. For excitation of erythrosin chromophores near 532 nm by the center of a TEM00 beam having a $1/e^2$ radius of R mm, the energy $E_{a=1}$ in microjoules corresponding to a value of $a = 1$ is 5.0 R^2. For a $1/e^2$ radius of 3.9 mm, a figure typical of many Nd:YAG lasers used in TPA experiments, this corresponds to a laser energy of 80 μJ per pulse. Phosphorescence can also be excited by an entire Gaussian beam of $1/e^2$ radius of R mm or by a circular beam of uniform profile having overall radius of R mm. In either case, the corresponding formula for $E_{a=1}$ is 10.0 R^2.

Measurements in the literature have been performed at reduced excitation energy densities both substantially above and below the value of 1 which we suggest. While published information on beam size and mode employed in specific studies is often incomplete, we have inferred a values ranging from 0.1 to over 600.[7,9,16-20] Clearly, the lower figure fails to define an anisotropy curve nearly as well as could be achieved with higher powers. The highest excitation energy, if actually employed, would have yielded phosphorescence anisotropies only 5% of the correct values, and so, in fact, lower energy densities were probably used. In general, published TPA results indicating unexpectedly low anisotropies for a particular phosphorescent probe ought to be carefully scrutinized for evidence of excitation saturation.

This discussion thus underscores the need to control carefully the excitation energy in TPA experiments. The extremely low phosphorescence signals available from cellular samples need to be maximized through adequate excitation, but depolarization due to saturation at excessive excitation energies must be carefully avoided. The data and calculations presented demonstrate that the range of excitation energies yielding truly optimum TPA data is surprisingly narrow.

ACKNOWLEDGMENTS

This work was supported in part by NIH Grant AI36306 to B.G.B.

REFERENCES

1. D. A. Axelrod (1983) *J. Membr. Biol.* **75**, 1–10.
2. G. M. Edelman (1976) *Science* **192**, 218–226.
3. M. Edidin (1974) *Annu. Rev. Biophys. Bioeng.* **3**, 179–201.
4. B. G. Barisas and T. R. Londo (1992) *SPIE Proc.* **1640**, 309–318.
5. T. R. Londo, N. A. Rahman, D. A. Roess, and B. G. Barisas (1993) *Biophys. Chem.* **48**, 241–257.
6. C. J. Philpott, N. A. Rahman, N. Kenny, T. R. Londo, R. M. Young, B. G. Barisas, and D. A. Roess (1995) *Biochim. Biophys. Acta* **1235**, 62–68.
7. R. Austin, S. Chan, and T. M. Jovin (1979) *Proc. Natl. Acad. Sci. USA* **76**, 5650–5654.
8. T. M. Jovin, M. Bartholdi, W. L. C. Vaz, and R. H. Austin (1981) *Ann. N.Y. Acad. Sci.* **366**, 176–196.
9. T. M. Jovin and W. L. C. Vaz (1989) *Meth. Enzymol.* **172**, 471–513.
10. J. R. Lakowicz (1983) *Principles of Fluorescence Spectroscopy*, Plenum Press, New York.
11. G. D. Johnson and E. J. Holborow (1986) in *Handbook of Experimental Immunology*, D. M. Weir (Ed.), Blackwell, Boston, vol. 1, Chap. 28.
12. T. R. Londo (1992) Ph.D. dissertation, Colorado State University, Fort Collins.
13. T. M. Yoshida, T. Jovin, and B. G. Barisas (1989) *Rev. Sci. Instrum.* **60**, 2924–2928.
14. J. R. Herman, T. R. Londo, N. A. Rahman, and B. G. Barisas (1992) *Rev. Sci. Instrum.* **63**, 5454–5458.
15. P. R. Bevington (Ed.) (1969) *Data Reduction and Error Analysis for the Physical Sciences,* McGraw–Hill, New York.
16. J. Gonzalez-Rodriguez, A. U. Acuna, M. V. Alvarez, and T. M. Jovin (1994) *Biochemistry* **33**, 266–274.
17. D. D. Thomas (1984) *J. Mol. Biol.* **179**, 55–81.
18. T. M. Eads, D. D. Thomas, and R. H. Austin (1984) *J. Mol. Biol.* **179**, 55–81.
19. R. H. Austin, J. Karohl, and T. M. Jovin (1983) *Biochemistry* **22**, 2082–3090.
20. K. Dornmair, A. F. Corin, J. K. Wright, and F. Jähnig (1985) *EMBO J.* **4**, 3633–3638.
21. E. H. Hellen and T. P. Burghardt (1994) *Biophys. J.* **66**, 891–897.